AFRL-AFOSR-JP-TR-2017-0003

Development of Advanced Li Rich xLi2MO3-(1-x)LiMO2 Composite Cathode for High Capacity Li Ion Batteries

Kuan-Zong Fung
NATIONAL CHENG KUNG UNIVERSITY

12/22/2016
Final Report

DISTRIBUTION A: Distribution approved for public release.

Air Force Research Laboratory
AF Office Of Scientific Research (AFOSR)/ IOA
Arlington, Virginia 22203
Air Force Materiel Command

REPORT DOCUMENTATION PAGE

Form Approved
OMB No. 0704-0188

The public reporting burden for this collection of information is estimated to average 1 hour per response, including the time for reviewing instructions, searching existing data sources, gathering and maintaining the data needed, and completing and reviewing the collection of information. Send comments regarding this burden estimate or any other aspect of this collection of information, including suggestions for reducing the burden, to Department of Defense, Executive Services, Directorate (0704-0188). Respondents should be aware that notwithstanding any other provision of law, no person shall be subject to any penalty for failing to comply with a collection of information if it does not display a currently valid OMB control number.

PLEASE DO NOT RETURN YOUR FORM TO THE ABOVE ORGANIZATION.

1. REPORT DATE *(DD-MM-YYYY)*	2. REPORT TYPE	3. DATES COVERED *(From - To)*
09-01-2017	Final	22 Sep 2015 to 21 Sep 2016

4. TITLE AND SUBTITLE
Development of Advanced Li Rich xLi2MO3-(1-x)LiMO2 Composite Cathode for High Capacity Li Ion Batteries

5a. CONTRACT NUMBER

5b. GRANT NUMBER
FA2386-15-1-4115

5c. PROGRAM ELEMENT NUMBER
61102F

6. AUTHOR(S)
Kuan-Zong Fung

5d. PROJECT NUMBER

5e. TASK NUMBER

5f. WORK UNIT NUMBER

7. PERFORMING ORGANIZATION NAME(S) AND ADDRESS(ES)
NATIONAL CHENG KUNG UNIVERSITY
1, TA HSUEH RD.,
TAINAN CITY, 70101 TW

8. PERFORMING ORGANIZATION REPORT NUMBER

9. SPONSORING/MONITORING AGENCY NAME(S) AND ADDRESS(ES)
AOARD
UNIT 45002
APO AP 96338-5002

10. SPONSOR/MONITOR'S ACRONYM(S)
AFRL/AFOSR IOA

11. SPONSOR/MONITOR'S REPORT NUMBER(S)
AFRL-AFOSR-JP-TR-2017-0003

12. DISTRIBUTION/AVAILABILITY STATEMENT
A DISTRIBUTION UNLIMITED: PB Public Release

13. SUPPLEMENTARY NOTES

14. ABSTRACT

Recently, lithium-rich layered oxides have become attractive cathode materials for high storage energy applications. Lithium rich layered oxides materials, represented by the general formula xLi2MnO3(1 - x)LiMO2 in which M is Mn, Ni and Co are of interest for both high-power and high capacity lithium ion cells. In this study, a series of cathode materials with chemical formula of xLi2MnO3(1-x)LiNi1/3Mn1/3Co1/3O2 (x = 0, 0.3, 0.5, 0.7 and 1.0) were synthesized by solgel method and investigated for their structure and electrochemical properties. The crystal structure of the sample was examined by X-ray diffraction. It is found that xLi2MnO3(1-x)LiNi1/3Mn1/3Co1/3O2 possessed the composite characteristic of two relatively similar layered structures. Its electrochemical performance is examined with galvanostatic charge/discharge. Increasing Li2MnO3 content tends to stabilize Li rich structure to increase capacity. On the other hand, Li2MnO3 shows an irreversible reaction with a reduced capacity. Accordingly, an optimized result was obtained from 0.5Li2MnO30.5LiNi1/3Mn1/3Co1/3O2 cathode which shows highest electrochemical performance with discharge capacity of 250 mAh/g. However, the capacity fading from these materials was also observed. To understand the behavior of capacity fading for Li-rich cathode materials, Li[Li0.2Mn0.54Ni0.13Co0.13]O2 as a cathode material for Li-ion battery has been carefully investigated. The result shows high initial charge capacity of 327 mAh/g and discharge capacity of 276 mAh/g at 0.05C rate (15mA/g) respectively. After 30 cycles, the discharge capacity decayed to 169 mAh/g. Transmission electron microscopy (TEM) images along with nano beam diffraction pattern (NDP) results showed the presence of spinel phases on the particles surface, indicating a phase transformation from layered to spinel-like structure. The electron diffraction analysis a

15. SUBJECT TERMS
Batteries, Electrodes, Cathodes, Composites, Lithium, Energy, Mesoporous, Failure Mechanism, Modeling, Oxygen Vacancy

16. SECURITY CLASSIFICATION OF:			17. LIMITATION OF ABSTRACT	18. NUMBER OF PAGES	19a. NAME OF RESPONSIBLE PERSON
a. REPORT	b. ABSTRACT	c. THIS PAGE			CASTER, KENNETH
Unclassified	Unclassified	Unclassified	SAR	17	**19b. TELEPHONE NUMBER** *(Include area code)* 315-229-3326

Standard Form 298 (Rev. 8/98)
Prescribed by ANSI Std. Z39.18

Development of Advanced Li Rich xLi_2MO_3-(1-x)$LiMO_2$ Composite Cathode for High Capacity Li Ion Batteries

October 2015 –September 2016

PI and Co-PI information:

Taiwan PI: Kuan-Zong Fung, National Cheng Kung University(NCKU)/ z8702009@email.ncku.edu.tw/Department of Materials Science and Engineering/ No.1, University Road, Tainan City 701, Taiwan (R.O.C.) /886-6-2380208

Co-PI: Chia-Chin Chang, National University of Tainan (NTUT)/ Department of Greenergy

US PI: Ying Shirley Meng, University of California San Diego(UCSD)/ Laboratory for Energy Storage and Conversion / Department of NanoEngineering

Period of Performance: October /1st/**2015** –**September** /30th/2016

Abstract:

Recently, lithium-rich layered oxides have become attractive cathode materials for high storage energy applications. Lithium rich layered oxides materials, represented by the general formula $xLi_2MnO_3 \cdot (1-x)LiMO_2$ in which M is Mn、Ni and Co are of interest for both high-power and high capacity lithium ion cells. In this study, a series of cathode materials with chemical formula of $xLi_2MnO_3(1-x)LiNi_{1/3}Mn_{1/3}Co_{1/3}O_2$ (x = 0, 0.3, 0.5, 0.7 and 1.0) were synthesized by sol–gel method and investigated for their structure and electrochemical properties. The crystal structure of the sample was examined by X-ray diffraction. It is found that $xLi_2MnO_3(1-x)LiNi_{1/3}Mn_{1/3}Co_{1/3}O_2$ possessed the composite characteristic of two relatively similar layered structures. Its electrochemical performance is examined with galvanostatic charge/discharge. Increasing Li_2MnO_3 content tends to stabilize Li rich structure to increase capacity. On the other hand, Li_2MnO_3 shows an irreversible reaction with a reduced capacity. Accordingly, an optimized result was obtained from $0.5Li_2MnO_30.5LiNi_{1/3}Mn_{1/3}Co_{1/3}O_2$ cathode which shows highest electrochemical performance with discharge capacity of 250 mAh/g. However, the capacity fading from these materials was also observed. To understand the behavior of capacity fading for Li-rich cathode materials, $Li[Li_{0.2}Mn_{0.54}Ni_{0.13}Co_{0.13}]O_2$ as a cathode material for Li-ion battery has been carefully investigated. The result shows high initial charge capacity of 327 mAh/g and discharge capacity of 276 mAh/g at 0.05C rate (15mA/g) respectively. After 30 cycles, the discharge capacity decayed to 169 mAh/g. Transmission electron microscopy (TEM) images

DISTRIBUTION A. Approved for public release: distribution unlimited.

along with nano beam diffraction pattern (NDP) results showed the presence of spinel phases on the particles surface, indicating a phase transformation from layered to spinel-like structure. The electron diffraction analysis and HRTEM images showing lattice distortion, the mechanism for capacity fading may provide better understanding of capacity fading in Li-rich composite cathodes.

Introduction:

Energy is important for all of the people because it is useful in our daily life. Methods to store and transport energy can be of great importance. Among advanced energy storage devices, lithium-ion batteries are remarkable systems due to their high energy density, high power density, and well cycled performance with considerable reliability. Lithium-ion batteries have been playing an important role in various application fields such as portable electronics and telecommunication equipments. In the past two decades, layered structure $LiCoO_2$ or $LiNi_{1/3}Mn_{1/3}Co_{1/3}O_2$(NMC) are known to be important cathode materials for many consumer electronics and auto applications. In a layer structured cathode formulated as $LiMO_2$, M^{+3} in is usually a transition metal ion, such as Mn, Co and Ni ions. During charging, Li+ is extracted out of the cation lattice accompanied by an electron moving toward the external circuit. Simultaneously, the trivalent M^{+3} will be oxidized to M^{+4} . As more and more Li ions are extracted, the screening effect becomes less effective. As a result, the strong repulsion from unscreened oxygen ions destabilizes the layer structure. Thus, the reversible capacity for layer structure is typically 50% of the theoretical capacity. In other words, only 50% of Li ions are allowed to be extracted from the Li cation sublattice.

Lu et al. [1] propose a interesting lithium rich layered oxide cathode materials (xLi_2MO_3- (1-x) $LiMO_2$, M = Mn, Co, Ni, Cr), The Li $[Li_{(1/3-2x/3)}Ni_xMn_{(2/3-x/3)}]O_2$ ($0 < x < 0.5$) system showed the very high capacity greater than 250mAh /g [2-3]. According to the workd conducted by Bo Xu et al study [4], Li_2MnO_3 is able to stabilize the MO_2 blocks in high capacity composite layered material xLi_2MO_3-(1-x) $LiMO_2$, by the rearrangement of Li ions occupying the transition metal layer as shown Fig.1 (a). As the lithium ions move out of the lithium layer in a layered structure, the lithium ions located in transition metal layers will move to the tetrahedral sites to stabilize the lithium layered structure, the schematic diagrams are shown in the following Figs.1(b) and (c).

DISTRIBUTION A. Approved for public release: distribution unlimited.

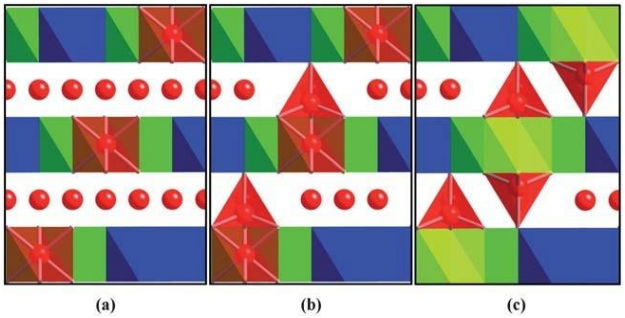

Fig.1 Sketch of Li–Li dumbbell formation (Red:Li; Green:Mn; Blue:Ni; Yellow: Vacancy). [4]

Although the xLi_2MnO_3•$(1-x)LiMO_2$ has very high theoretical capacity and has been regarded as the next-generation cathode material for LIBs, they still exhibit problems such as (1) capacity fading upon cycling, (2) low rate capability. Therefore, the main objective of this work is to (1) study the electrochemical behavior Li rich layered composite cathode xLi_2MO_3-$(1-x)LiMO_2$ derived from adequate nanotechnology, (2) study the influence of surface modification on the capacity fading of xLi_2MO_3-$(1-x)LiMO_2$ layered cathode, (3) investigate the importance of mesoporous nanostructure on high-rate behavior of Li rich layered composite cathode (4) conduct the modeling and calculation of xLi_2MO_3-$(1-x)LiMO_2$ layered cathode with variation in surface modification and porous structure. The main tasks for the 1st year include materials synthesis and electrochemical testing (**NCKU-NUTN**) and computational modeling of layered composite xLi_2MO_3-$(1-x)LiMO_2$ **(UC-SD).**

Experimental:

Powder preparation

In this study, the $0.5Li_2MnO_3$-$0.5LiNi_{1/3}Mn_{1/3}Co_{1/3}O_2$ powders were prepared by sol–gel method using citric acid monohydrate as the chelating agent. At first, lithium acetate, manganese (II) acetate tetrahydrate, nickel (II) acetate hexahydrate and cobalt (II) acetate hexahydrate were dissolved in deionize water with the addition of an aqueous solution of citric acid. Then, ethylene glycol was further added into the prepared solution with continuous stirring. The molar ratio of total metal ions to citric acid was 1:1. The resultant solution was evaporated at 120℃ until a sol was obtained. As the water evaporated further, the sol turned into a viscous gel. The resulting gel precursors were pre-calcined at 450℃ for 4 hours in air to

DISTRIBUTION A. Approved for public release: distribution unlimited.

eliminate the organic substances. The pre-calcined powders were calcined at 900℃ for 12 hours in the air, and then furnace-cooled to room temperature to obtain the final oxide powders.

X-ray diffraction

Powder X-ray diffraction (Rigaku D-max) with Cu-Kα radiation was used to identify the crystalline phase of the final oxide powders. The XRD spectra were collected in a range of 2θ values from 10^o to 70^o at a scanning rate of 0.5 degrees per min and a step size of 0.02^o.

Scanning electron microscope

The morphology of final oxide powders were characterized by scanning electron microscope (SEM, Hitachi, S3000).

Elemental Analysis

The elemental analysis was conducted by an inductively coupled plasma-mass spectrometer (ICP-MS).

Electrochemical Characterization

The working electrodes were prepared by mixing the synthesized sample, carbon black and poly-vinylidene fluoride at a weight ratio of 80:10:10 in the solvent of N-methylpyrrolidone. The resulting slurries were cast onto aluminum current collectors and then dried at 100℃ under vacuum for 24 hours. The foils were rolled to thin sheets, then cut into disks with a diameter of 13 mm. CR2032 coin-type cells were assembled in an argon-filled glove box, and lithium foils were used as counter electrodes, and polypropylene microporous films were used as separators. The electrolyte consisted of 1 M $LiPF_6$ in a mixture of ethyl carbonate and diethyl carbonate at a 1:1 volume ratio. The galvanostatic charge and discharge tests were carried out on a Arbin testing instrument in a voltage range between 2.0V and 4.8V at 0.1C rate (30mA/g).

Transmission electron microscopy

Transmission electron microscopy (TEM) and nano beam diffraction pattern (NDP) were performed using a JEOL JEM-2100F CS-STEM at 200 kV. TEM specimens of the pristine material were prepared by dispersing the powder in ethanol and adding a few drops of the resulting suspension to a holey TEM copper grid. For cycled materials, the powders were removed from the electrode, ground, dispersed in ethanol, and sonicated for 10–15 minutes. Few drops of the solution were added to the holey Cu grid for TEM observation. Electron diffraction patterns were simulated by CaRIne Crystallography 3.1 using the unit cell of the $LiMO_2$ structure with $R\bar{3}m$ space group and the Li_2MnO_3 structure with C2/m space group, and

DISTRIBUTION A. Approved for public release: distribution unlimited.

the spinel structure with Fd$\bar{3}$m space group.

Results and Discussion:

1. Phase identification of $0.5Li_2MnO_3$-$0.5LiNi_{1/3}Mn_{1/3}Co_{1/3}O_2$ powders

Fig. 2 shows the X-ray diffraction patterns of $0.5Li_2MnO_3$-$0.5LiNi_{1/3}Mn_{1/3}Co_{1/3}O_2$ prepared at 900 ℃. The XRD patterns of Li_2MnO_3 and $LiNi_{1/3}Mn_{1/3}Co_{1/3}O_2$ (NMC) are indexed as C2/m and R$\bar{3}$m respectively. The Si peak was used to calibrate XRD data. There is no detectable impurity phase in the whole scan 2θ range, indicating that the $0.5Li_2MnO_3$-$0.5LiNi_{1/3}Mn_{1/3}Co_{1/3}O_2$ was successfully synthesized from the sol-gel method.

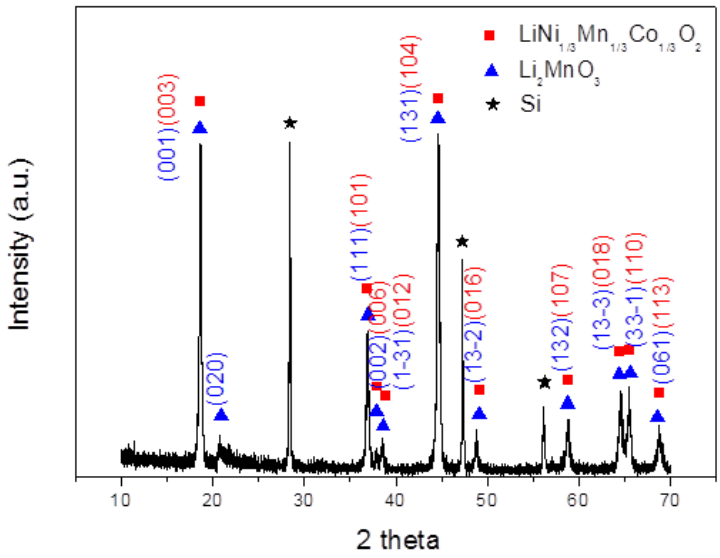

Fig 2. XRD pattern of $0.5Li_2MnO_3$-$0.5LiNi_{1/3}Mn_{1/3}Co_{1/3}O_2$ prepared by sol-gel method

2. Morphology and ICP-AES analysis of .$5Li_2MnO_3$-$0.5LiNi_{1/3}Mn_{1/3}Co_{1/3}O_2$ powders

Fig 3 shows the SEM image of $0.5Li_2MnO_3$-$0.5LiNi_{1/3}Mn_{1/3}Co_{1/3}O_2$ prepared by sol-gel method. The powder shows semi-spherically shaped and the particles are non-agglomerated. Fig.3 shows the particle size distribution of the powder. The average size of the particle is about 214.5 nm. The particle size distribution result matches well with the morphology observe on SEM image

DISTRIBUTION A. Approved for public release: distribution unlimited.

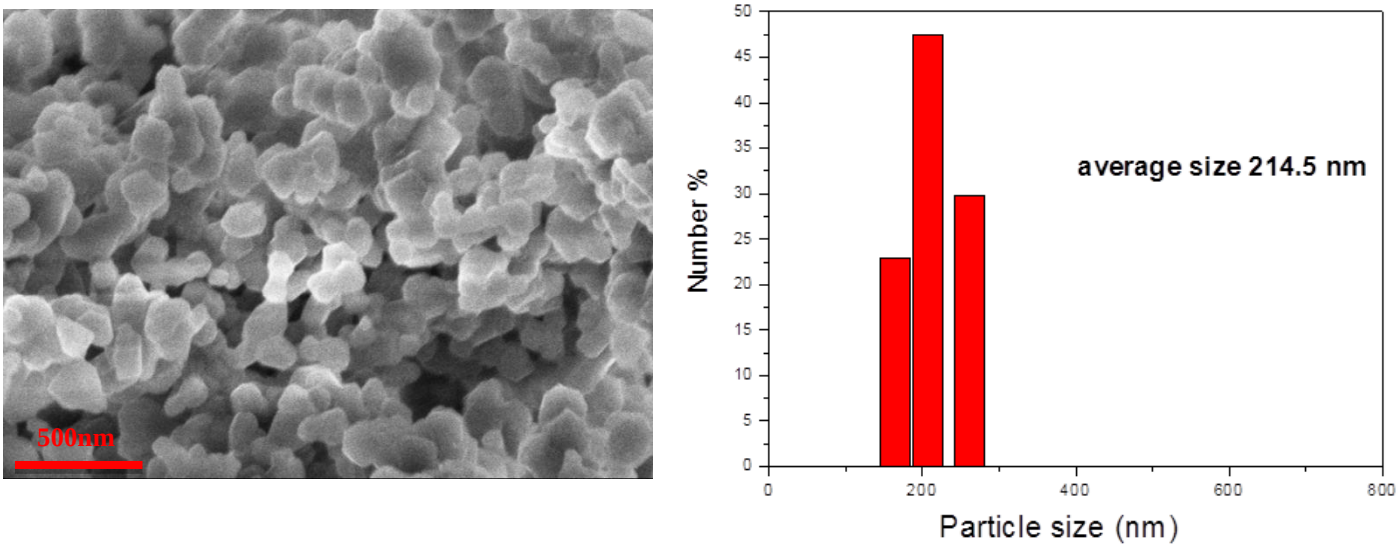

Fig3.SEM image and particle size distribution of $0.5Li_2MnO_3$-$0.5LiNi_{1/3}Mn_{1/3}Co_{1/3}O_2$ powder

$0.5Li_2MnO_3$-$0.5LiNi_{1/3}Mn_{1/3}Co_{1/3}O_2$ may be expressed in another form – $Li_{1.2}Mn_{0.54}Ni_{0.13}Co_{0.13}O_2$. The stoichiometry of the synthesized cathode material is confirmed by the inductively coupled plasma-mass spectrometer (ICP-MS) analysis. Table 1 shows the chemical composition from the ICP analysis is found to be consistent with the stoichiometry of the prepared powders.

Table 1. Chemical composition results from inductively coupled plasma emission spectrometry (ICP) analysis of $Li_{1.2}Mn_{0.54}Ni_{0.13}Co_{0.13}O_2$

	Li	Mn	Ni	Co
Ideal values	1.2	0.533	0.133	0.133
Observed values	1.20704	0.52908	0.13179	0.13210

3. Electrochemical performance of $0.5Li_2MnO_3$-$0.5LiNi_{1/3}Mn_{1/3}Co_{1/3}O_2$ powders

The charge-discharge profiles of $Li_{1.2}Mn_{0.54}Ni_{0.13}Co_{0.13}O_2$ in Fig.3 (a) show the 1st, 2nd, 15th and 30th cycles. As demonstrated in Fig.3(a), the as-prepared cathode material suggest that the first charge and discharge capacity are 327 mAh/g and 276 mAh/g,

DISTRIBUTION A. Approved for public release: distribution unlimited.

respectively, resulting in an irreversible capacity loss of 51 mAh/g. In Fig3.(b), the electrochemical reaction of the initial charge process can be divided into two dominant stages: step I and II.

Step I shows a similar charge-discharge profile similar to that of $LiMn_{0.33}Co_{0.33}Ni_{0.33}O_2$ (NMC). This is due to the removing of Li from the NMC part in $Li_{1.2}Mn_{0.54}Ni_{0.13}Co_{0.13}O_2$ electrode with oxidation of TM ions ($Co^{3+/4+}$ and $Ni^{2+/4+}$), with Mn remaining as Mn^{4+}. Step II exhibits a long voltage plateau at 4.5V, which is corresponding to the oxygen loss during the charging of Li_2MnO_3. Interestingly, this voltage plateau disappears in second charge profiles. This result reveals that the oxygen loss is an irreversible process. Based on the calculation of capacity of lithium rich layered oxide from extracting more electrons from lattice, the formation of oxygen vacancy from oxygen release is necessary. These phenomena have been also observed by other researchers. [5, 6, 7]

Fig.3(c) shows the cyclic performance of $Li_{1.2}Mn_{0.54}Ni_{0.13}Co_{0.13}O_2$ cathode tests in 0.05C rate. The discharge capacity faded from 276mAh/g to 169mAh/g after 30cycles. The capacity retention is about 62%.

(a)

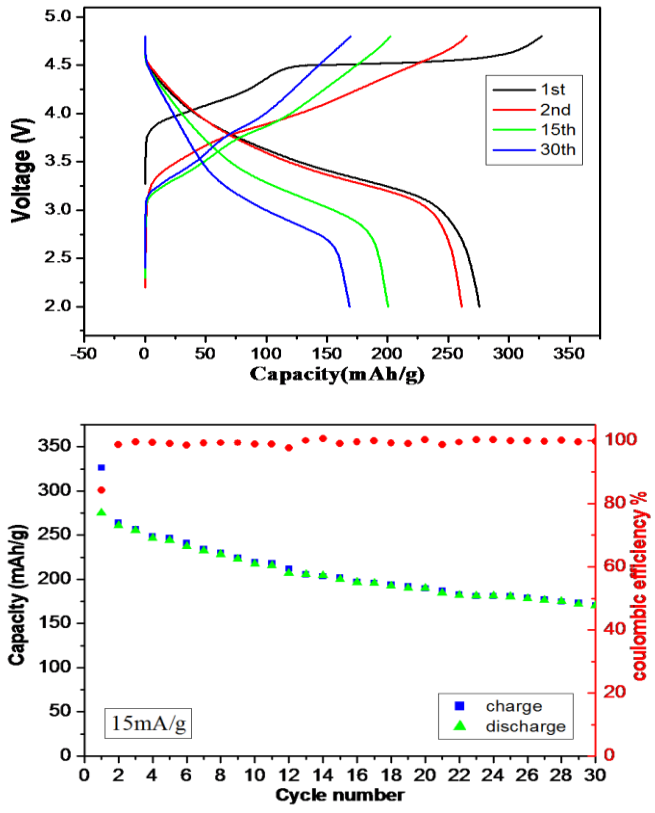

(b)

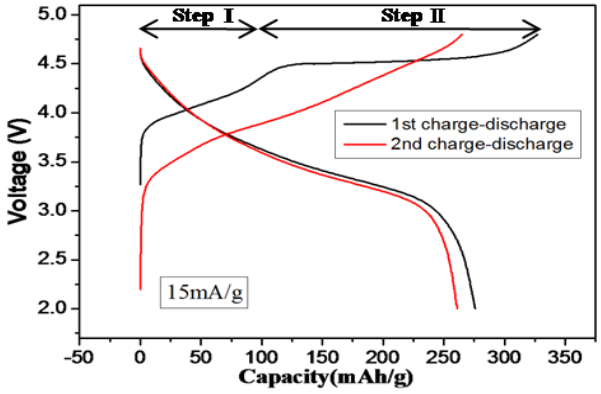

Fig 4. (a),(b)charge-discharge curve and (c) cyclic performance of $Li_{1.2}Mn_{0.54}Ni_{0.13}Co_{0.13}O_2$

DISTRIBUTION A. Approved for public release: distribution unlimited.

4. Phase transformation of $Li_{1.2}Mn_{0.54}Ni_{0.13}Co_{0.13}O_2$

To understand the causes for the capacity fading on cycled layered composite cathode material, TEM analysis was conducted. From observation of TEM diffraction pattern of $Li_{1.2}Mn_{0.54}Co_{0.13}Ni_{0.13}O_2$ powder, more detail information about the structural change may be obtained.

4-1 TEM image of $Li_{12}Mn_{0.54}Ni_{0.13}Co_{0.13}O_2$ before cycling

Transmission electron microscopy (TEM) analyses were performed to observe the cathode powder. Figs 5. (a)(b) show that the pristine sample is well-crystallized particle with a particle size about 240 nm. Figs 5. (c) and (d) showed simulated electrical diffraction pattern of $LiMO_2$ ($R\bar{3}m$) along the [$\bar{4}41$] zone axis and Li_2MnO_3 (C2/m) along the [$10\bar{1}$] zone axis. Accordingly, we can accurately analyze the NDP pattern from a pristine $Li_{12}Mn_{0.54}Ni_{0.13}Co_{0.13}O_2$ particle shown in Fig.5 (b) The bright diffraction spots represent the (104) plane and (110) plane of the $LiMO_2$ ($R\bar{3}m$) which is marked as red circle. It is noted that these bright fundamental diffraction spots also overlap with (131) plane and (060) plane of the Li_2MnO_3 (C2/m) which is marked as green circle. The zone axis of NDP pattern of pristine $Li_{1.2}Mn_{0.54}Ni_{0.13}Co_{0.13}O_2$ is along the [$\bar{4}41$] zone and [$10\bar{1}$] zone for $LiMO_2$ ($R\bar{3}m$) and Li_2MnO_3 (C2/m), respectively. The weak diffraction spots may be indexed as (020) and (040) for superlattice domain between Li and TM ions in the TM layers, from a Li_2MnO_3 domain, respectively.

4-2 TEM image of $Li_{1.2}Mn_{0.54}Ni_{0.13}Co_{0.13}O_2$ after cycling

The TEM image of cycled $Li_{1.2}Mn_{0.54}Ni_{0.13}Co_{0.13}O_2$ powder from both the center and surface regions is shown in Fig. 6 (a). Nano beam diffraction pattern (NDP) was taken from center "b" in Fig. 6(a). There are three weak diffraction spots between the bright diffraction spots shown in Fig. 6(b). To analyze these diffraction points, ED pattern of $LiMn_2O_4$ and Li_2MnO_3 are simulated as shown in Fig. 6(c)(d). According to Fig. 6(d) and 6(f), the weak diffraction spots represent (020) and (040) planes of Li_2MnO_3-like phase and (022) plane of spinel-like phase in center region. Comparing to the surface, only one weak diffraction point between the bright diffraction spots is detected and shown in Fig. 6(c). Furthermore, the peak intensities integrated from the selected area diffraction in the center and surface region are shown in Fig. 6(d) and 6(e). The elimination of (020) and (040) diffraction spots from Li_2MnO_3 phase suggests that Li_2MnO_3 transformed into a $LiMn_2O_4$ phase.

DISTRIBUTION A. Approved for public release: distribution unlimited.

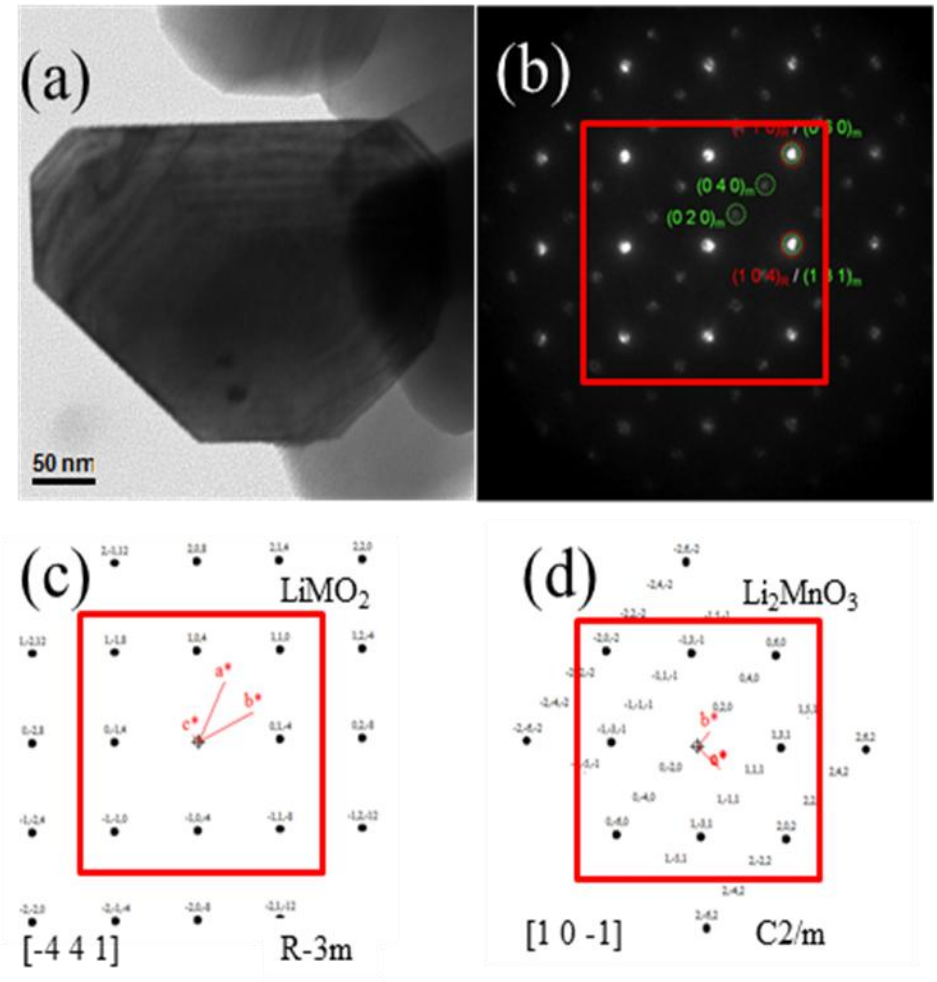

Fig 5. **(a)** TEM bright filed image of pristine $Li_{1.2}Mn_{0.54}Ni_{0.13}Co_{0.13}O_2$ particle **(b)** nano beam diffraction pattern (NDP) shows mixture of layered $LiMO_2$ and Li_2MnO_3 which are consistent with simulated patterns **(c)** and **(d)**

DISTRIBUTION A. Approved for public release: distribution unlimited.

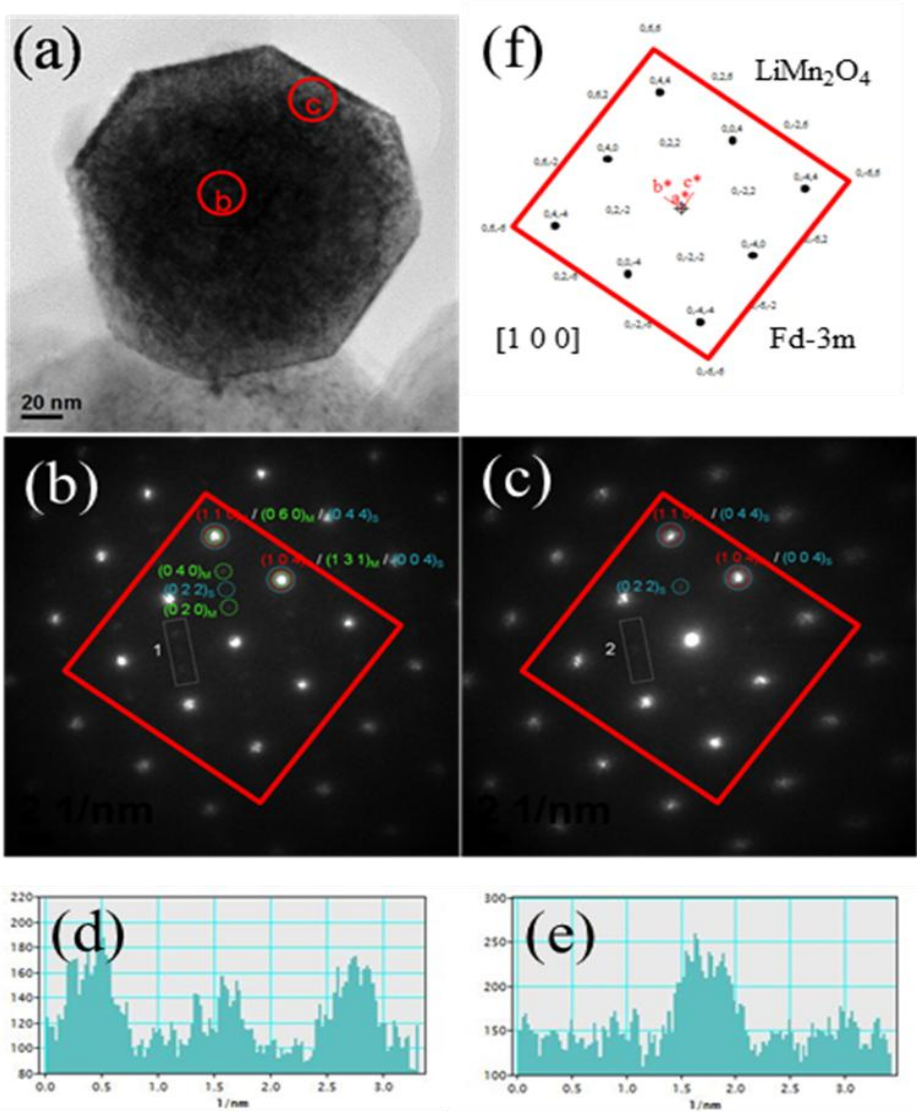

Fig 6. **(a)** TEM bright filed image of cycled $Li_{1.2}Mn_{0.54}Ni_{0.13}Co_{0.13}O_2$ particle Nano beam diffraction patterns (NDP) were taken from **(b)** center and **(c)** outer regions of the particle. From SAED intensity profile shown in **(d)** and **(e)**, it is suggested that the center of the particle still shows Li_2MnO_3-like layered structure; however, the outer region has changed to a spinel-like ($LiMn_2O_4$, $Fd\bar{3}m$) pattern.

DISTRIBUTION A. Approved for public release: distribution unlimited.

4-3 Phase evolution of $Li[Li_{0.2}Mn_{0.54}Ni_{0.13}Co_{0.13}]O_2$

Before charge-discharge tests, the $Li[Li_{0.2}Mn_{0.54}Ni_{0.13}Co_{0.13}]O_2$ particles showed cation-ordering peaks, indicating the ordered arrangement of one Li and two Mn in the TM layers, corresponding to Li_2MnO_3-like phase. After charge-discharge tests, the diffraction spots from newly formed spinel-like phase were observed in both Fig. 6 (b) and Fig.6 (c). The intensity of cation-ordering peaks of cycled particles decreases in comparison to pristine particles. These results suggest that spinel phase formed on the surface.

Therefore, phase transformation is the main reason of capacity fading. Formation of spinel phase causes the insertion/extraction of some lithium ions no longer reversible. Fig.7. Shows the possible phase transformation mechanism of $Li_{1.2}Mn_{0.54}Ni_{0.13}Co_{0.13}O_2$.

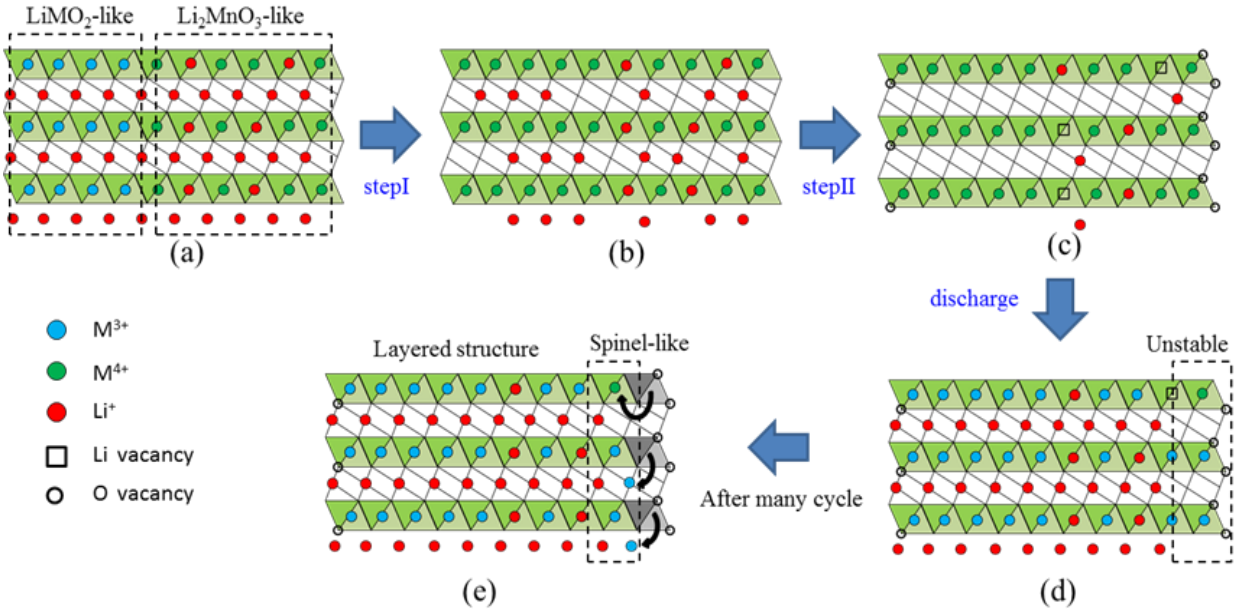

Fig 7. Scheme of the phase transformation for $Li_{1.2}Mn_{0.54}Ni_{0.13}Co_{0.13}O_2$ powder explaining structure evolutions observed between the pristine material and cycled powder.

4-4 Approaches for Improvement of Layered Composite Cathode

In order to use lithium rich layered oxide cathode material for practical applications, how to minimize its capacity fading is one important task. Based on our TEM and electrochemical test result, phase transformation of $Li_{1.2}Mn_{0.54}Ni_{0.13}Co_{0.13}O_2$ from layered to spinel is the main reason why capacity fading takes place. Phase transformation in $Li_{1.2}Mn_{0.54}Ni_{0.13}Co_{0.13}O_2$ is caused by the oxygen release and vacancy formation during the charge-discharge. The suppression of oxygen release and formation of oxygen vacancies in

DISTRIBUTION A. Approved for public release: distribution unlimited.

$Li_{1.2}Mn_{0.54}Ni_{0.13}Co_{0.13}O_2$ is very crucial to obtain a stable layer structure and then minimize the capacity fading through long-term cycling tests. Approach to suppress the formation of excessive oxygen vacancies or oxygen loss through substitutions of other elements in transition metal layer is an effective way to minimize capacity fading [8-10].

The USCD research group applied First principles computation to investigate the effects of cation substitution on the oxygen vacancy formation energy in high energy density $0.5Li_{4/3}Mn_{2/3}O_2 \cdot 0.5LiNi_{1/2}Mn_{1/2}O_2$ cathode material.

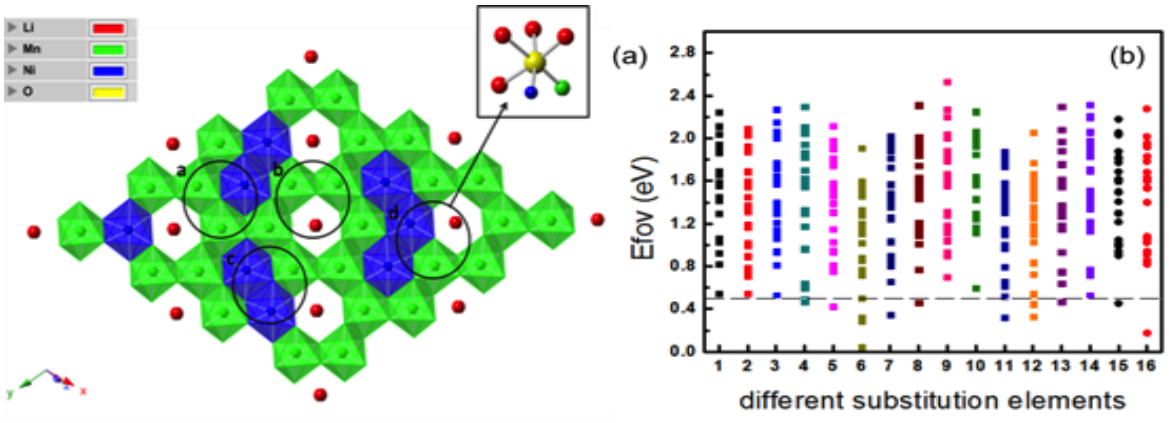

Fig. 8. (a) cation ordering in transition metal layer: $0.5Li_{4/3}Mn_{2/3}O_2 \cdot 0.5LiNi_{1/2}Mn_{1/2}O_2$. (b) oxygen vacancy formation energy of $Li_{8/12}Ni_{3/12}Mn_{6/12}M_{1/12}O_2$ at different configurations. #1 is the model without substitution.

Fig. 8(a) shows the cation ordering in the transition metal layer: Li ions (in red color), Mn ions (in green color), and Ni ions (in blue color), there are two different Li sites; one is surrounded by six Mn-ions, the other is surrounded by five Mn ions and one Ni-ion. Since Ni-ions contribute to the reversible capacity, we substitute one of Mn-ions with different cations. From our previous study, as Li is extracted from the structure, the oxygen vacancy formation energy decreased drastically. Figure 7(b) shows the oxygen vacancy formation energy as a function of different substitution elements. It can be seen that elements #9 and # 10 enhanced the oxygen stability in the lattice.

With computational results of UCSD collaborator based on the density of state and electronic structure of the candidate materials, NCKU team will conduct and verify the optimal composition for the high-capacity composite cathode with better performances in next year.

DISTRIBUTION A. Approved for public release: distribution unlimited.

Conclusions

(1) Li-rich cathode materials $0.5Li_2MnO_3$-$0.5LiNi_{1/3}Mn_{1/3}Co_{1/3}O_2$ were successfully synthesized. This study suggested that$0.5Li_2MnO_3$-$0.5LiNi_{1/3}Mn_{1/3}Co_{1/3}O_2$ possessed the composite characteristic.

(2) The electrochemical performance of $0.5Li_2MnO_3$-$0.5LiNi_{1/3}Mn_{1/3}Co_{1/3}O_2$ electrodes indicated that Li_2MnO_3 may stabilize Li rich structure. These factors resulted that $0.5Li_2MnO_3$-$0.5LiNi_{1/3}Mn_{1/3}Co_{1/3}O_2$ cathode exhibited best electrochemical performance with discharge capacity 250 mAh/g.

(3)The degradation mechanism of the $0.5Li_2MnO_3$-$0.5LiNi_{1/3}Mn_{1/3}Co_{1/3}O_2$ electrode during charge-discharge test is investigated by combined derivation of reaction equation and TEM structural analysis. Our results indicate that the structural degradation occurred mainly on the surface of the materials where the phase transformation from layer to spinel is dominant.

Reference:

1.Holdren, J.P., Energy and sustainability. SCIENCE-NEW YORK THEN WASHINGTON-, 2007. 315(5813): p. 737.

2.Ginley, D., M.A. Green, and R. Collins, Solar energy conversion toward 1 terawatt. Mrs Bulletin, 2008. 33(04): p. 355-364.

3.Tarascon, J.-M. and M. Armand, Issues and challenges facing rechargeable lithium batteries. Nature, 2001. 414(6861): p. 359-367.

4.Armand, M. and J.-M. Tarascon, Building better batteries. Nature, 2008. 451(7179): p. 652-657.

5.Kang, K. and G. Ceder, Factors that affect Li mobility in layered lithium transition metal oxides. Physical Review B, 2006. 74(9): p. 094105.

6.Jeong, J.-H., et al., The influence of compositional change of 0.3 Li 2 MnO 3· 0.7 LiMn 1− x Ni y Co 0.1 O 2 (0.2≤ x≤ 0.5, y= x− 0.1) cathode materials prepared by co-precipitation. Journal of Power Sources, 2011. 196(7): p. 3439-3442.

7.Wang, Y., et al., High capacity spherical Li[Li0.24Mn0.55Co0.14Ni0.07]O2 cathode material for lithium ion batteries. Solid State Ionics, 2013. 233: p. 12-19.

DISTRIBUTION A. Approved for public release: distribution unlimited.

8.X. Jin, Q.J. Xu, H.M. Liu, X.L. Yuan, Y.Y. Xia, Electrochem Acta 136 (2014) 19.
9. Y. Wu, A. Manthiram, Solid State Ionics, 180, 50–56 (2009).
10. J. M. Zheng, Z. R. Zhang, X. B. Wu, Z. X. Dong, Z. Zhu and Y. Yang, J. Electrochem. Soc., 155, A775–A782 (2008).

List of Publications and Significant Collaborations that resulted from your AOARD supported project: In standard format showing authors, title, journal, issue, pages, and date, for each category list the following:

(c) Conference presentations

1. *K. Z. Fung, S. Y. Tsai , C. T. Ni , W. Z. Lin, and B. Y. Huang,* Understanding of Capacity Loss/Fading of Li-Rich Layer-Structured Cathode Materials Based on Structural/Electrochemical Analyses, 229th ECS Meeting, May 29 - June 2, 2016, San Diego, CA
2. *K. Z. Fung, C. T. Ni , W. Z. Lin, and B. Y. Huang,* Study of Capacity Fading of Li-Rich Layer-Structured Cathode Materials Based on Structural and Electrochemical Analyses, 2016 International Conference on Green Electrochemical Technologies, Sep 21-23, 2016, Taipei, TAIWAN
3. Kuan-Zong Fung, Shu-Yi Tsai, Chung-Ta Ni, Bo-Yuan Huang, "Investigation of Capacity Fading of Li-rich Layered Composite Cathodes based on Structure Considerations," Materials Science & Technology 2016, Oct. 23-27, 2016, Salt Lake City, UT

Abstract for 229th ECS Meeting,

Li-rich layer-structured cathode materials formulated as xLi_2MnO_3 -(1-x)$LiMO_2$(M = Mn, Ni, Co, etc.) have received much attention due to their surprisingly high reversible capacity for Li-ion battery applications. For the understanding of these materials, a systematic study on complicated crystal structures and reaction mechanisms during electrochemical charge/discharge cycles is employed. Although Li-rich layer-structured cathode material show a reversible capacity as high as 250 mAh/g at low rate, its electrochemical properties such as capacity loss at first cycle, rate capability and capacity fading still need to be examined and characterized. In this study, several compositions of xLi_2MnO_3 -(1-x)$LiMO_2$ (M = Mn, Ni, Co, etc.) were investigated. The TEM structural analysis shows that the evidence of spinel phase after cycling. It is believed

that the transition from layered structure to spinel structure may induce a large lattice distortion resulting in lattice breakdown and capacity. In additions, the phase transition is caused by the redox reaction of transition metal ions through charging/discharging tests. Thus, the cycling behavior of Li-rich layer-structured oxides is studied by changing the oxidation state of transition metal ions in the layered structures. XRD, SEM, TEM will be used for characterization of cycled cathode materials.

Abstract for Materials Science & Technology 2016

The cathode capacity of layered oxides have been improved from 140 mAh/g (for LiCoO2) to 180 mAh/g (for Li(Ni0.8Co0.15Al0.05)O2). Recently, Li-rich layer structured composite cathode formulated as xLi_2MnO_3 (1-x)- $LiMO_2$ (M = Mn, Ni, Co, etc.) exhibit reversible capacity as high as 250 mAh/g for Li-ion battery applications. However, its electrochemical properties such as capacity loss at first cycle, rate capability and capacity fading upon cycling still need to be investigated. A systematic study on crystal structures and electrochemical testing is employed. In this study, certain compositions of xLi_2MnO_3 (1-x)- $LiMO_2$ (M = Mn, Ni, Co, etc.) were investigated. The electron diffraction pattern of spinel structure was observed from a cycled layer structured cathode particle. The phase transition from layered structure to spinel structure may induce large lattice distortion resulting in lattice breakdown and capacity fading. Discussion will be carried out based on the results of XRD, SEM, TEM analysis on cycled cathode materials.

DD882: As a separate document, please complete and sign the inventions disclosure form.

Important Note: If the work has been adequately described in refereed publications, submit an abstract as described above but cite important findings to your above List of Publications, and if possible, attach any reprint(s) as an appendix. If a full report needs to be written, then submission of a final report that is very similar to a full length journal article will be sufficient in most cases.